IV. GRAVITY SURVEY

Takemi Ishihara, Fumitoshi Murakami, Teruki Miyazaki,
and Kiyokazu Nishimura

Introduction

Gravity measurements on some of the islands in the survey area have been made by the Geographical Survey Institute and some Japanese academic researchers (e.g. FUJII *et al.*, 1964; TANAKA *et al.*, 1974; OHKAWA and YOKOYAMA, 1977). Gravity measurements with surface ship gravimeters have been made during cruises of research vessels belonging to both the Ocean Research Institute and United States and some free air anomaly maps have been published (TOMODA, 1973; SEGAWA and TOMODA, 1976; SEGAWA and BOWIN, 1976; WATTS, 1976). These previous measurements have revealed the general characteristics of gravity anomalies over the Izu-Ogasawara island arc system, but the first intensive survey with a high density of measurements was performed during cruises GH79-2, GH79-3 and GH79-4.

Gravity Measurements

Gravity measurements during these cruises were obtained with a LaCoste-Romberg air-sea gravimeter S-63 on a gyrostabilized platform, with cross-coupling corrections and satellite navigation for exact location. The data processing procedures used are the same as for previous cruises (e.g. MIYAZAKI, 1979).

S-63 gravimeter readings and meter-zero values at ports are listed in Table

Table IV-1 S-63 gravimeter readings at ports during GH79-2, GH79-3 and GH79-4 cruises

CRUISE	PORT	ABSOLUTE GRAVITY VALUE*	DATE	GRAVITY READING	METER ZERO
GH79-2	Funabashi	979789.38	Apr. 16, 1979	10696.4	969101.5
	Futami (Chichijima)	979441.74**	May 3	10351.6	969098.4
	Funabashi	979789.38	May 15	10701.8	969096.1
GH79-3	Funabashi		May 28	10703.7	969094.2
	Funabashi		July 6	10706.0	969091.9
GH79-4	Funabashi		July 13	10708.6	969089.4
	Okada (Oshima)	979855.38***	Aug. 5	10775.3	969088.7
	Funabashi	979789.38	Aug. 11	10709.1	969088.9

*Absolute gravity value in milligals at mean sea level tied to IGSN 71.

**Tied to the gravity station in the office of the Chichijima weather station (absolute gravity value 979439.44 mgal).

***Tied to the gravity station in the office of the Oshima weather station (absolute gravity value 979808.57 mgal).

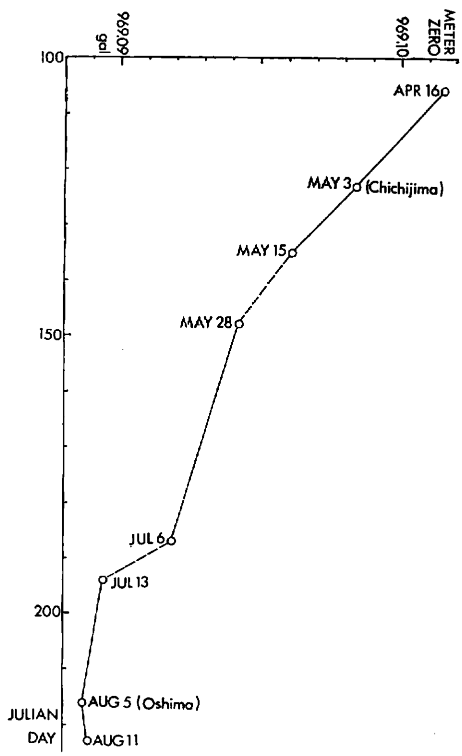

Fig. IV-1 Meter-zero curve for LaCoste-Romberg air-sea gravimeter S-63 during cruises GH79-2, 3 and 4.

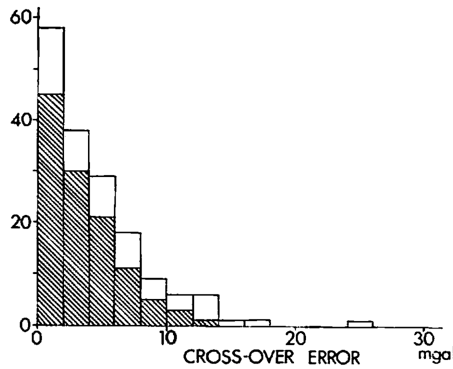

Fig. IV-2 Histogram of discrepancy between observed free air anomalies at intersection of the ship's tracks. The hatched area indicates intersections where observed anomalies change more slowly than at the rate of one mgal/min along both of the tracks, and the white area indicates other intersections.

IV-1 (for explanation of a meter-zero value see NETTLETON, 1976, p. 122–124). Absolute gravity values at Futami Port, Chichijima Island and at Okada Port, Oshima Island were calculated by comparing measurements made with a Worden land gravimeter with those at stations of the Japan Gravity Standardization Net 1975 (Geographical Survey Institute, 1976). Fig. IV-1 shows that the meter-zero values decreased rather steadily but the rate of decrease became slower from cruise to cruise: the average drift rate is 5.6, 1.8, 0.5 mgal/month for cruises GH79-2, GH79-3 and GH79-4 respectively.

In order to estimate the accuracy of the gravity measurements of these cruises, the discrepancies between observed free air anomalies at intersections of the ship's tracks are given in a form of a histogram (Fig. IV-2). The white area in Fig. IV-2 indicates cases in which the free air anomaly value along at least one of the intersecting tracks changes at a rate of more than one mgal/min, i.e. at a rate of more than 3.2 mgal/km when the ship's speed was 10 kt. It is obvious from this figure that the discrepancy is generally greater when the free air anomaly value changes rapidly, which suggests that these discrepancies are due in a considerable part to errors in navigation. A total of 167 discrepancies show a standard deviation of 5.8 mgal, while the standard deviation decreases to 4.5 mgal for 116 discrepancies at the intersections where the free air anomaly values along both of the tracks change at a rate of less than one mgal/min (the hatched area in Fig. IV-2).

Characteristics of Free Air Anomalies

Fig. IV-3 shows the free air anomalies in the survey area. Profiles of the free air, simple Bouguer, and magnetic anomalies, as well as the topography along each survey line, are given in Fig. IV-4.

In general, topographic highs such as the Shichito Ridge, the Ogasawara Ridge, the Izu Ridge, the Mariana Ridge, and the West Mariana Ridge are associated with high free air anomalies, while topographic lows such as the Ogasawara Trench, the Mariana Trench, the Ogasawara Trough and the Mariana Trough are associated with low anomalies. The trends of the topographic features and those of the gravity anomalies agree well, but the amplitude of the free air anomalies varies less regularly.

For the sake of convenience, we divide the survey area into four provinces, and describe the characteristics of each province separately.

The Northern Mariana Region [up to lat 24°N, L1 to L11, Fig. IV-4]

The northernmost part of the Mariana Trough is characterized by positive anomalies generally in the range of +30 to +70 mgal, with maxima in the center and minima near both its eastern and western edges.

The Mariana Ridge east of the Mariana Trough is associated with positive anomalies generally greater than +80 mgal with maxima up to +130 mgal on active or historically active shallow volcanic seamounts. Gravimetrically, the West Mariana Ridge is similar to the Mariana Ridge, with positive anomalies generally greater than +80 mgal. Two belts of high anomalies extend northward and northeastward from the Mariana Ridge. These belts are also noticeable topographically.

Minimum values of free air anomalies (up to −220 mgal) occur at about 24°N in the Mariana Trench.

The Ogasawara-Iwojima Region [lat 24°N to lat 30°N, L12 to L32, Fig. IV-4]

Free air anomalies exceed +150 mgal around all the volcanic islands along the Shichito Ridge: Minami-Iwojima, Iwojima, Kita-Iwojima Islands. A gravity survey was carried out near Nishinoshima Island during a previous cruise (Ishihara, 1977) and gravity measurements were obtained on Nishinoshima Island (Ohkawa and Yokoyama, 1977), and these results also show maximum free air anomaly values of up to +190 mgal around Nishinoshima Island. Anomalies along the rest of the Shichito Ridge are much lower than around the volcanic islands, generally having values in the range +60 to +100 mgal.

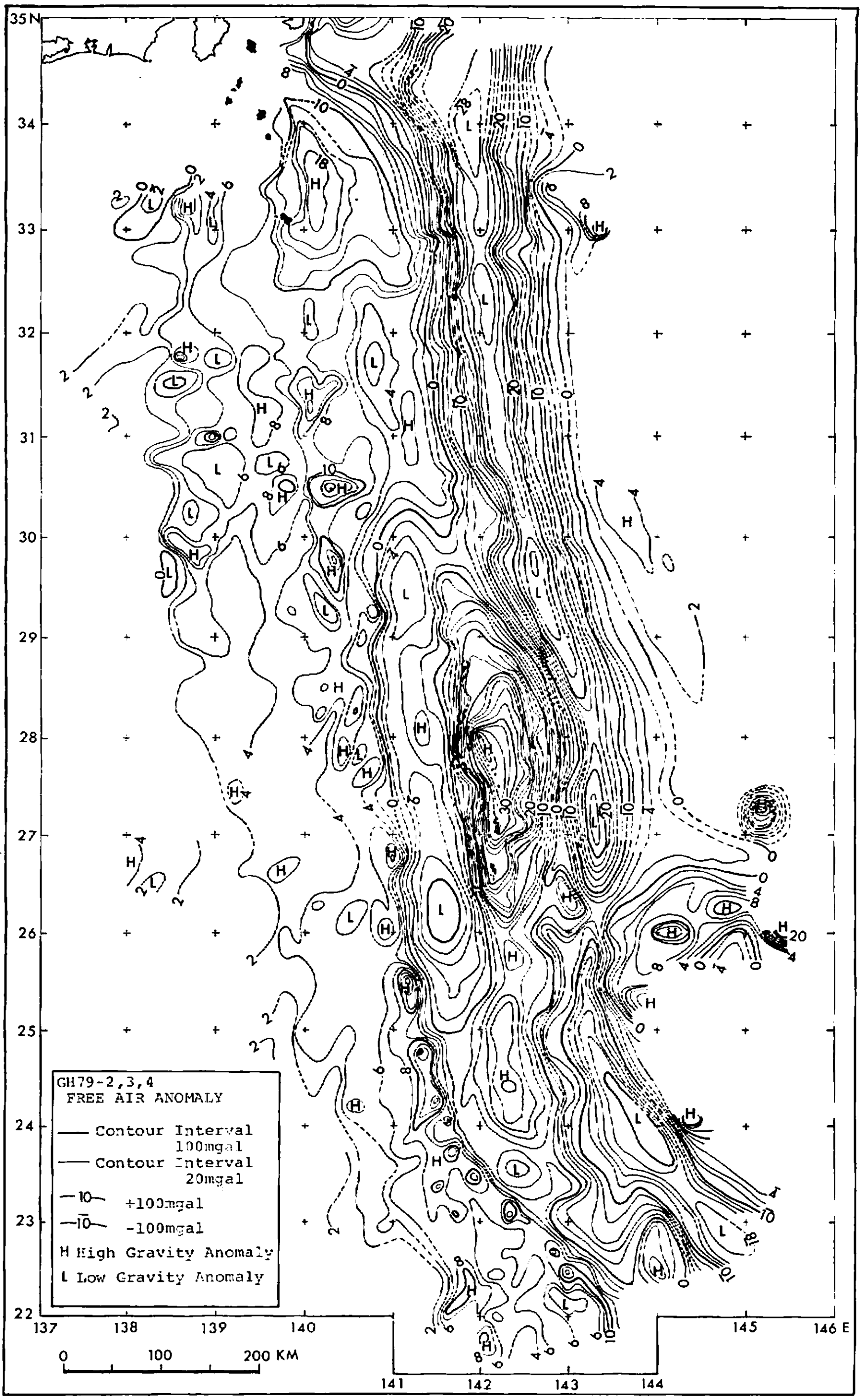

Fig. IV-3 Free air anomalies in the survey area.

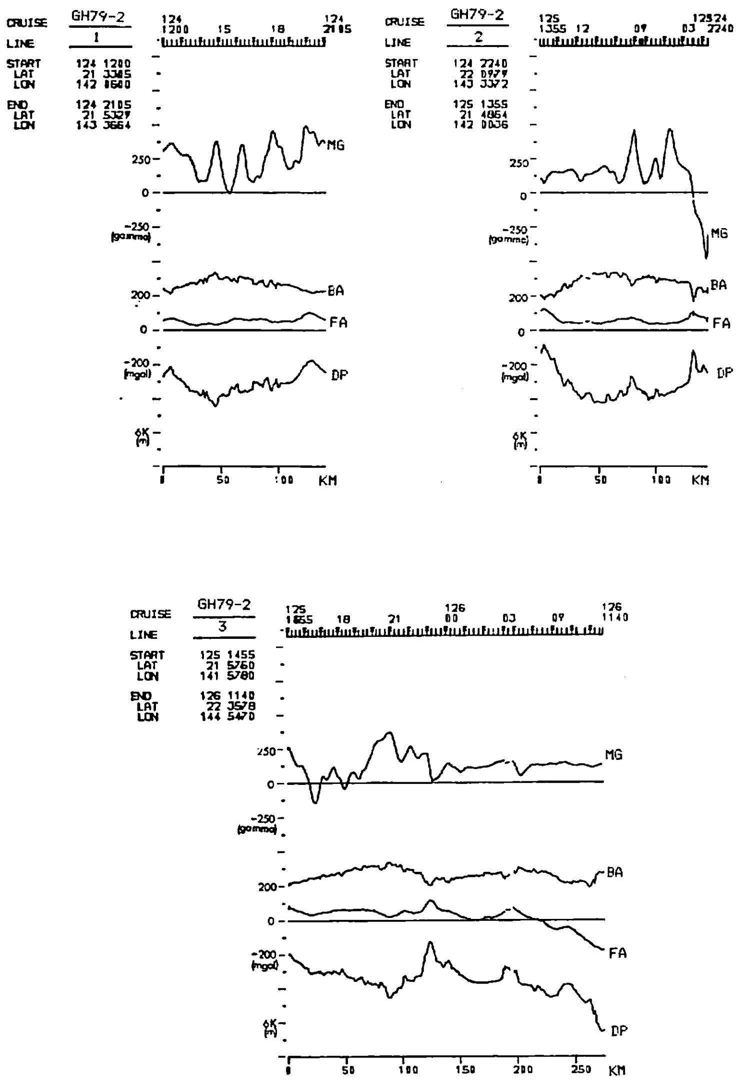

Fig. IV-4 (A)

Fig. IV-4 Profiles of free air, simple Bouguer, magnetic anomalies and topography along the survey lines.

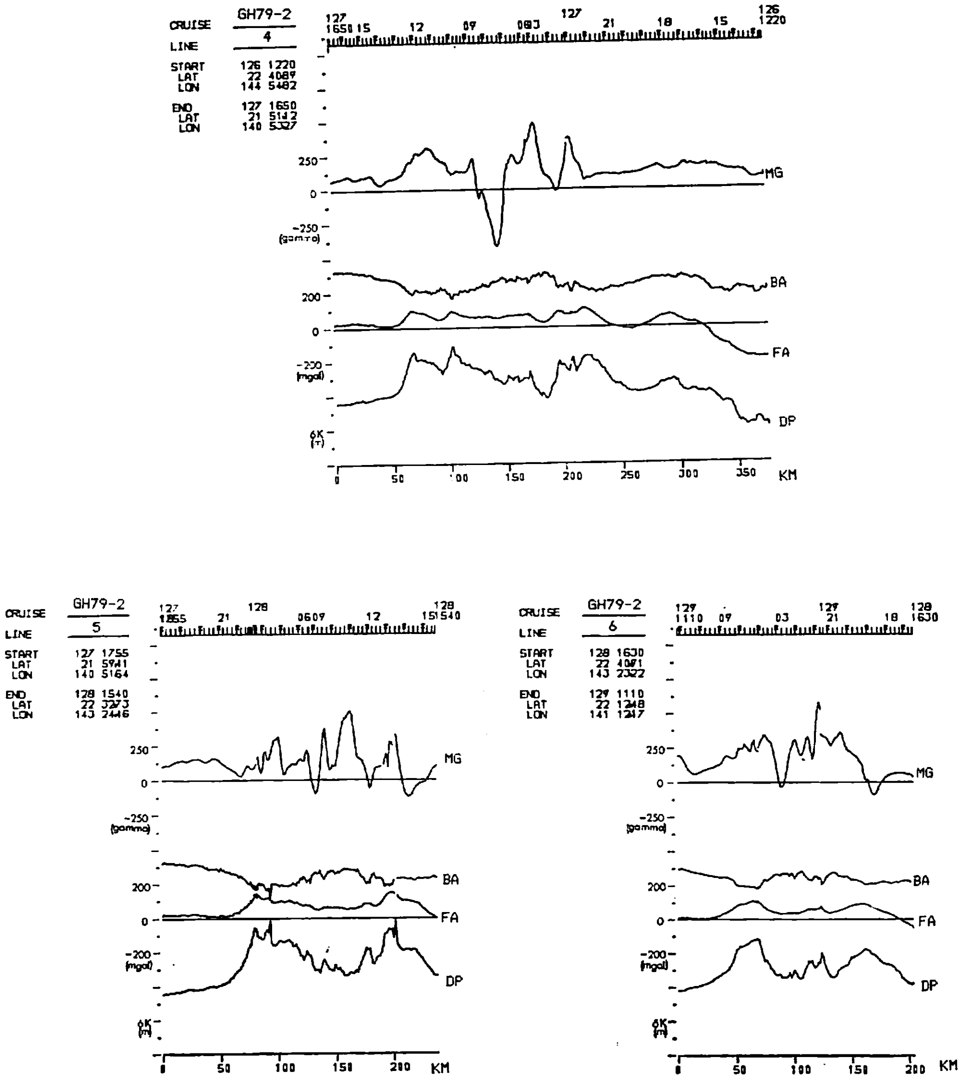
CRUISE GH79-2
LINE 4
START 126 1220
LAT 22 4089
LON 144 5482
END 127 1650
LAT 21 5142
LON 140 5327
MG
BA
FA
DP
KM
CRUISE GH79-2
LINE 5
START 127 1755
LAT 21 5941
LON 140 5164
END 128 1540
LAT 22 3273
LON 143 2446
CRUISE GH79-2
LINE 6
START 128 1630
LAT 22 4081
LON 143 2322
END 129 1110
LAT 22 1248
LON 141 1247

Fig. IV-4 (B)

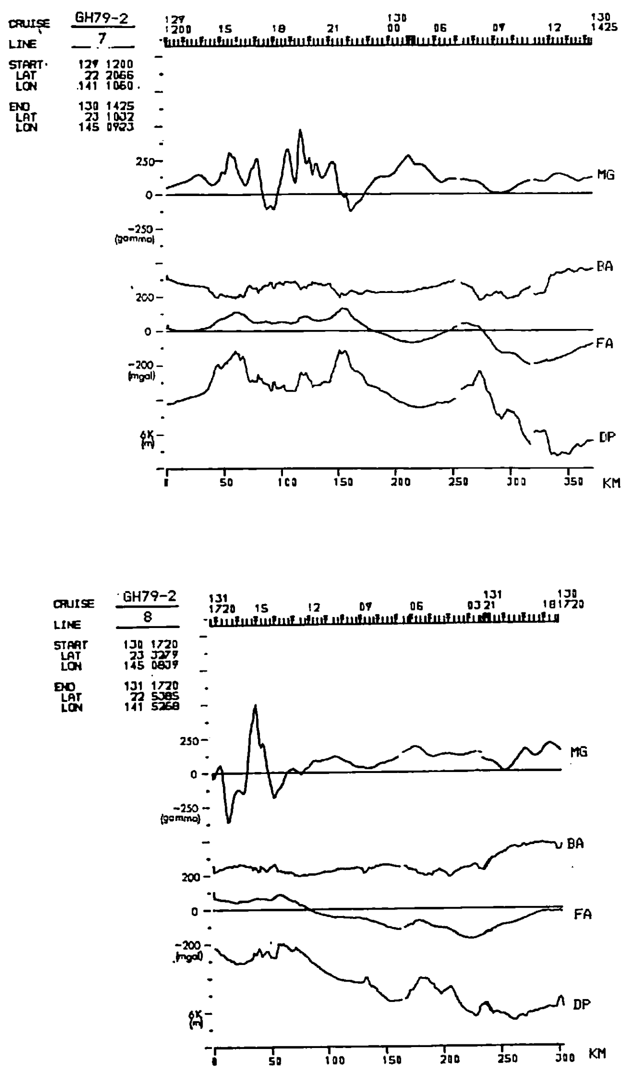
CRUISE GH79-2
LINE 7
START 129 1200
LAT 22 2066
LON 141 1060
END 130 1425
LAT 23 1032
LON 145 0923
250
0
-250 (gamma)
MG
BA
200
0
-200 (mgal)
FA
DP
50 100 150 200 250 300 350 KM
CRUISE GH79-2
LINE 8
START 130 1720
LAT 23 3279
LON 145 0839
END 131 1720
LAT 22 5385
LON 141 5268
250
0
-250 (gamma)
MG
BA
200
0
-200 (mgal)
FA
DP
50 100 150 200 250 300 KM

Fig. IV-4 (C)

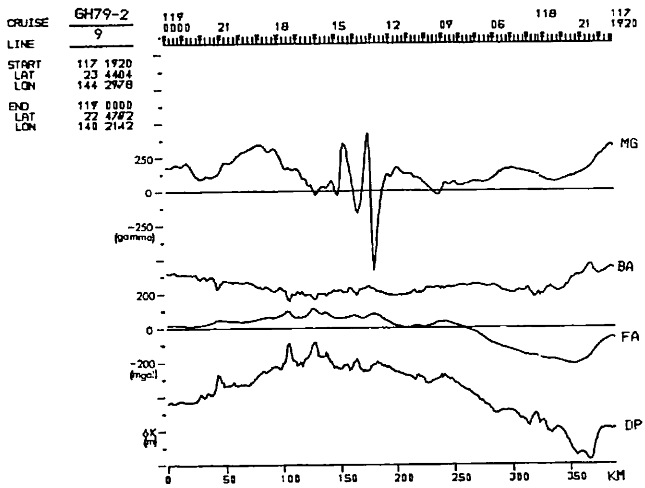
CRUISE GH79-2
LINE 9
START 117 1920
LAT 23 4404
END 119 0000
LON 140 2142
MG
250
0
-250
(gamma)
BA
200
0
FA
-200
(mgal)
DP
0
50
100
150
200
250
300
350
KM

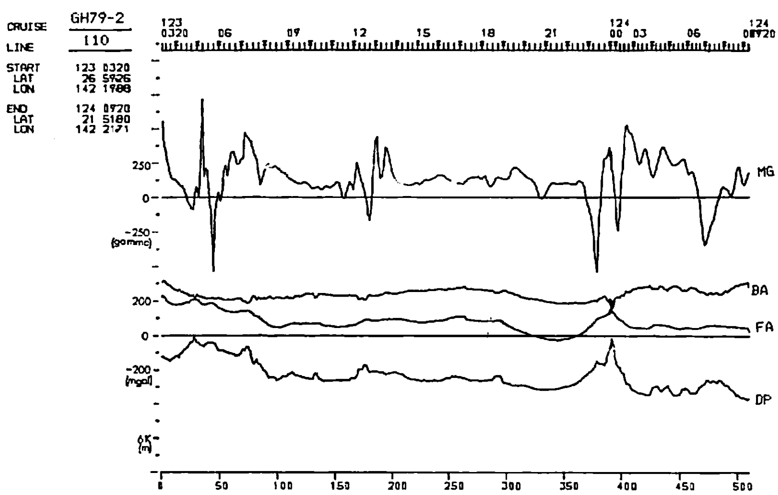
CRUISE GH79-2
LINE 110
START 123 0320
LAT 26 5926
END 124 0920
LAT 21 5180
MG
250
0
-250
(gamma)
BA
200
0
FA
-200
(mgal)
DP
0
50
100
150
200
250
300
350
400
450
500

Fig. IV-4 (D)

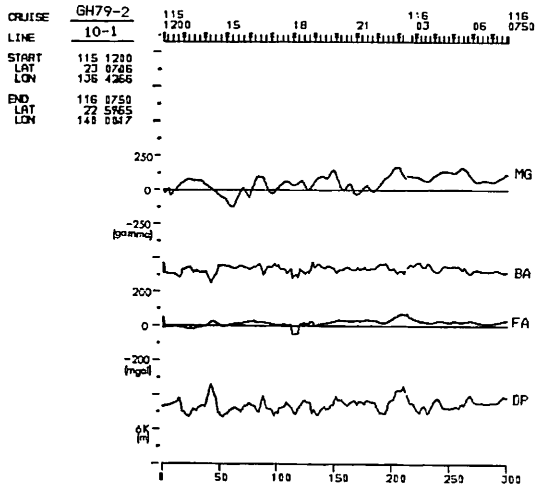

CRUISE
GH79-2
LINE
10-1
START
115 1200
LAT
23 0706
LON
136 4266
END
116 0750
LAT
22 5965
LON
140 0017
115 1200
15
18
21
116 03
06
116 0750
250
0
-250
(gamma)
MG
200
0
-200
(mgal)
BA
FA
DP
6K
(m)
0
50
100
150
200
250
300

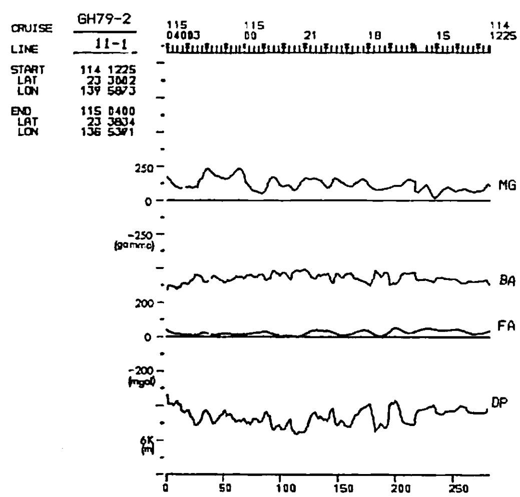

CRUISE
GH79-2
LINE
11-1
START
114 1225
LAT
23 3002
LON
139 5873
END
115 0400
LAT
23 3834
LON
136 5371
115 0400
115 00
21
18
15
114 1225
250
0
-250
(gamma)
MG
200
0
-200
(mgal)
BA
FA
DP
6K
(m)
0
50
100
150
200
250

Fig. IV-4 (E)

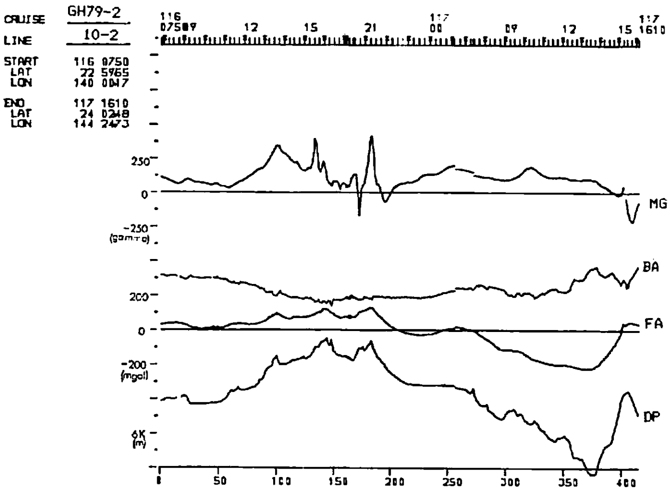
CRUISE GH79-2
LINE 10-2
START 116 0750
LAT 22 5965
LON 140 0047
END 117 1610
LAT 24 0248
LON 144 2473
MG
BA
FA
DP
250
0
-250
(gamma)
200
-200
(mgal)
6K
(m)

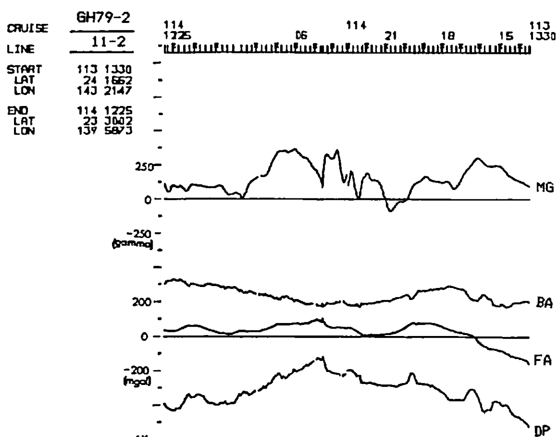
CRUISE GH79-2
LINE 11-2
START 113 1330
LAT 24 1662
LON 143 2147
END 114 1225
LAT 23 3002
LON 139 5873
MG
BA
FA
DP
250
0
-250
(gamma)
200
-200
(mgal)
6K
(m)

Fig. IV-4 (F)

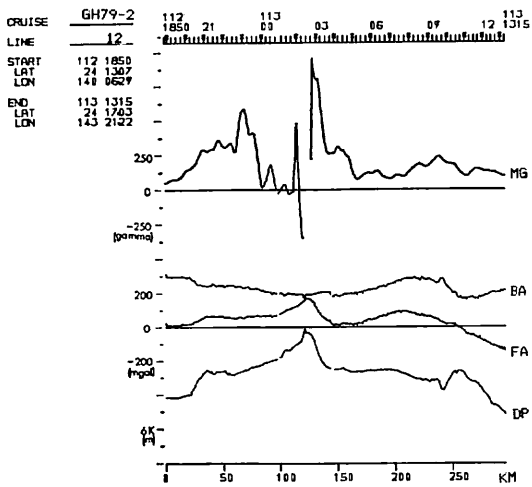
CRUISE GH79-2
LINE 12
START
LAT
LON
END
LAT
LON
MG
BA
FA
DP
(gamma)
(mgal)
KM

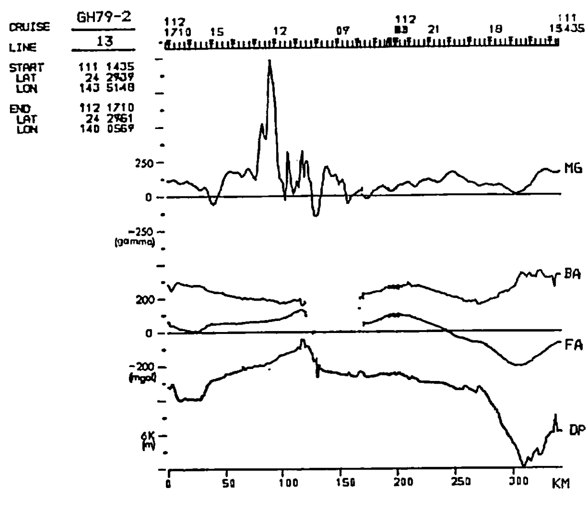
CRUISE GH79-2
LINE 13
START
LAT
LON
END
LAT
LON
MG
BA
FA
DP
(gamma)
(mgal)
KM

Fig. IV-4 (G)

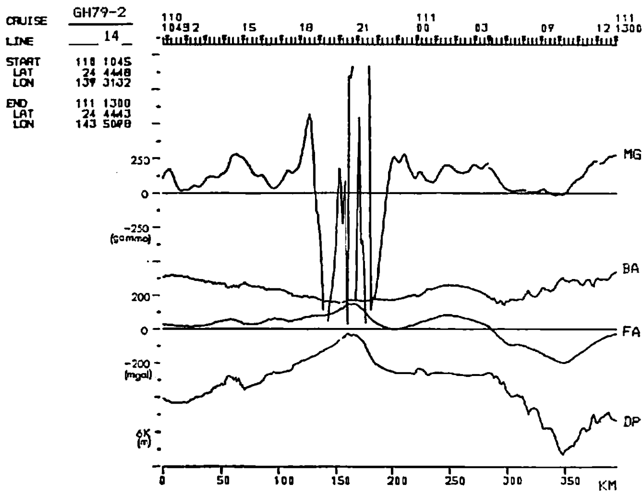
CRUISE GH79-2
LINE 14
START 110 1045
LAT 24 4448
LON 139 3132
END 111 1300
LAT 24 4443
LON 143 5098
250
0
-250
(gamma)
200
0
-200
(mgal)
6K
(m)
MG
BA
FA
DP
0
50
100
150
200
250
300
350
KM

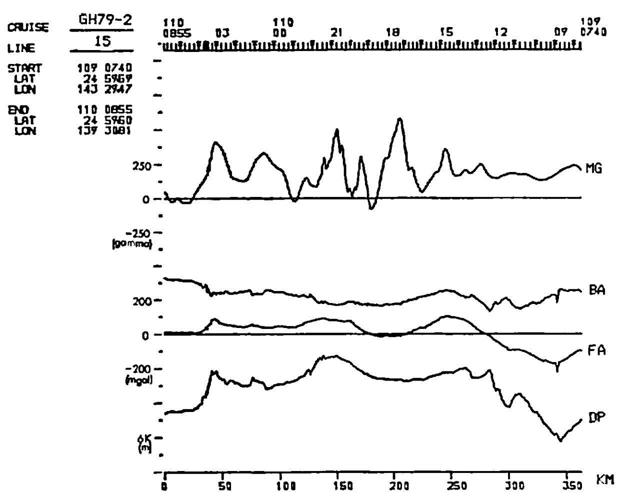
CRUISE GH79-2
LINE 15
START 109 0740
LAT 24 5969
LON 143 2947
END 110 0855
LAT 24 5960
LON 139 3081
250
0
-250
(gamma)
200
0
-200
(mgal)
6K
(m)
MG
BA
FA
DP
0
50
100
150
200
250
300
350
KM

Fig. IV-4 (H)

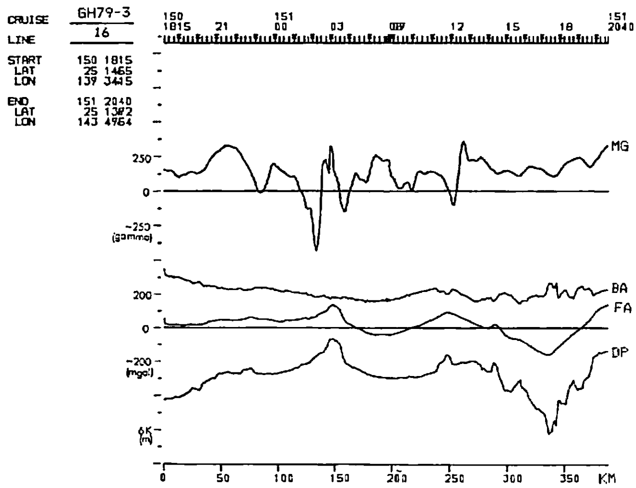
CRUISE
GH79-3
LINE
16
START
150 1815
LAT
LON
END
151 2040
LAT
LON
MG
BA
FA
DP
250
0
-250
(gamma)
200
0
-200
(mgal)
6K
(m)
0
50
100
150
200
250
300
350
KM

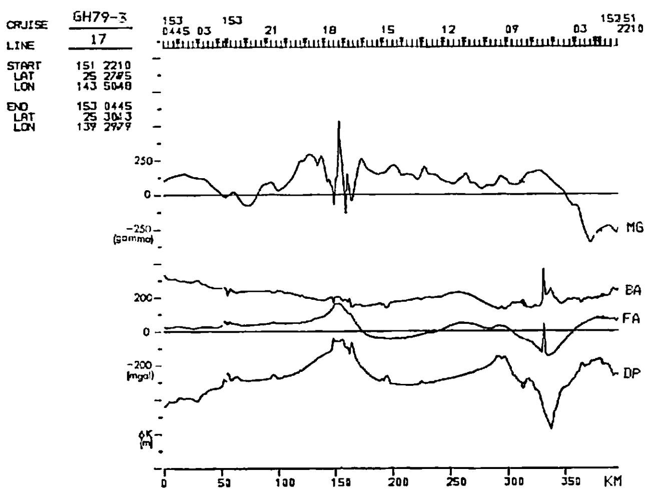
CRUISE
GH79-3
LINE
17
START
151 2210
LAT
LON
END
153 0445
LAT
LON
MG
BA
FA
DP
250
0
-250
(gamma)
200
0
-200
(mgal)
6K
(m)
0
50
100
150
200
250
300
350
KM

Fig. IV-4 (I)

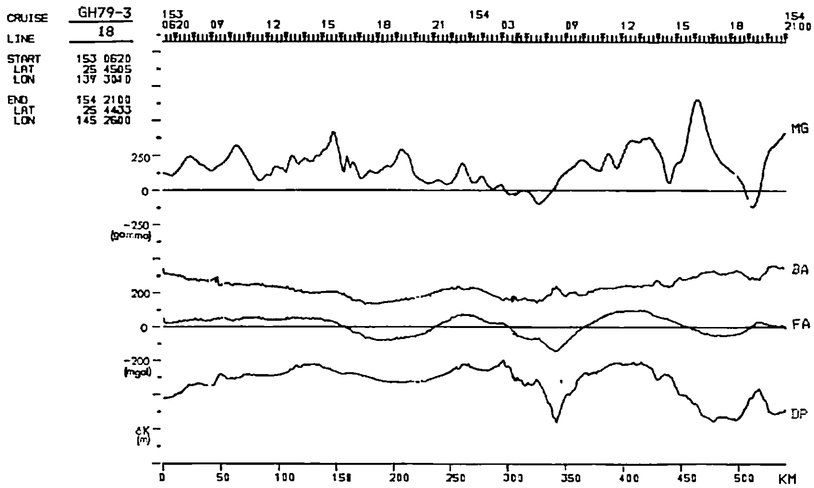
CRUISE GH79-3
LINE 18
START 153 0620
LAT 25 4505
LON 139 3040
END 154 2100
LAT 25 4433
LON 145 2600
MG
BA
FA
DP
250
0
-250
(gamma)
200
0
-200
(mgal)
6K
(m)
KM

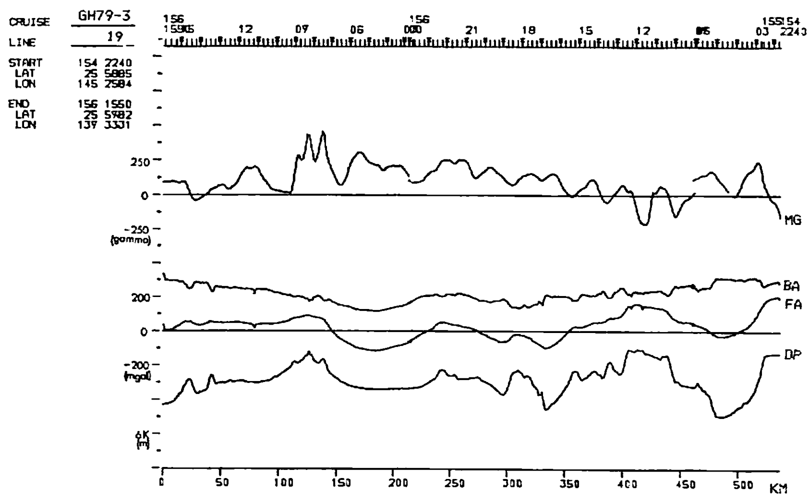
CRUISE GH79-3
LINE 19
START 154 2240
LAT 25 5885
LON 145 2584
END 156 1550
LAT 25 5982
LON 139 3331
MG
BA
FA
DP
250
0
-250
(gamma)
200
0
-200
(mgal)
6K
(m)
KM

Fig. IV-4 (J)

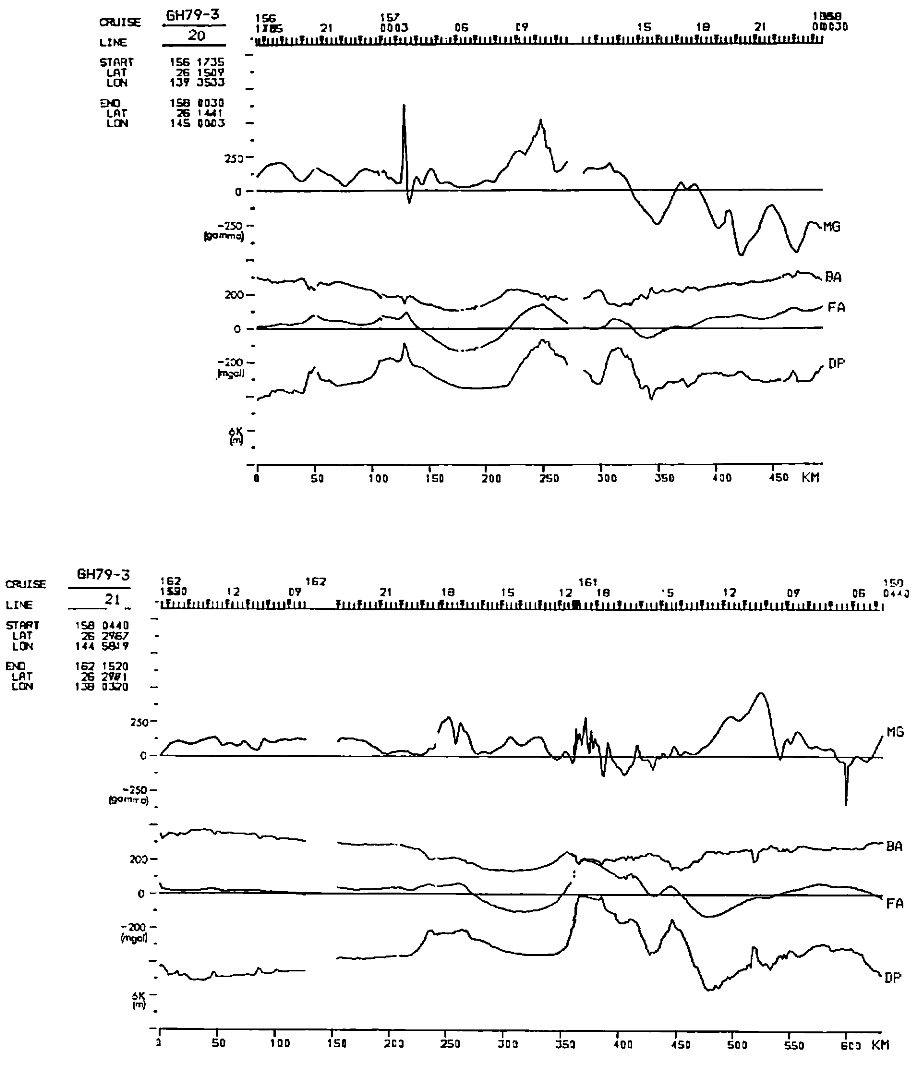
CRUISE
GH79-3
LINE
20
START
LAT
LON
156 1735
26 1509
139 3533
END
LAT
LON
158 0030
26 1441
145 0003
250
0
-250
(gamma)
MG
BA
200
FA
0
-200
(mgal)
DP
6K
(m)
0
50
100
150
200
250
300
350
400
450 KM
CRUISE
GH79-3
LINE
21
START
LAT
LON
158 0440
END
LAT
LON
162 1520
250
0
-250
(gamma)
MG
BA
200
0
FA
-200
(mgal)
DP
6K
(m)
0
50
100
150
200
250
300
350
400
450
500
550
600 KM

Fig. IV-4 (K)

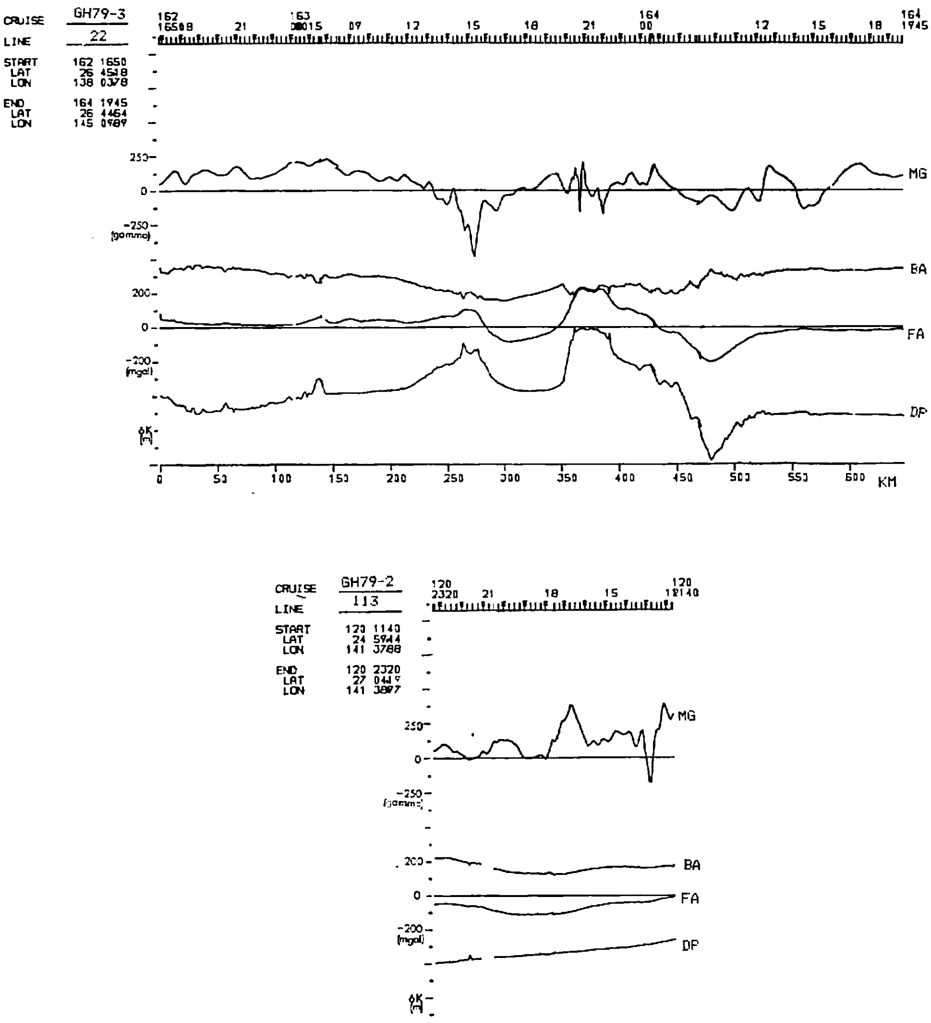
CRUISE GH79-3
LINE 22
START 162 1650
LAT 26 4518
LON 138 0378
END 164 1945
LAT 26 4464
LON 145 0989
MG
BA
FA
DP
(gamma)
(mgal)
KM
CRUISE GH79-2
LINE 113
START 120 1140
LAT 24 5944
LON 141 3788
END 120 2320
LAT 27 0419
LON 141 3897
MG
BA
FA
DP
KM

Fig. IV-4 (L)

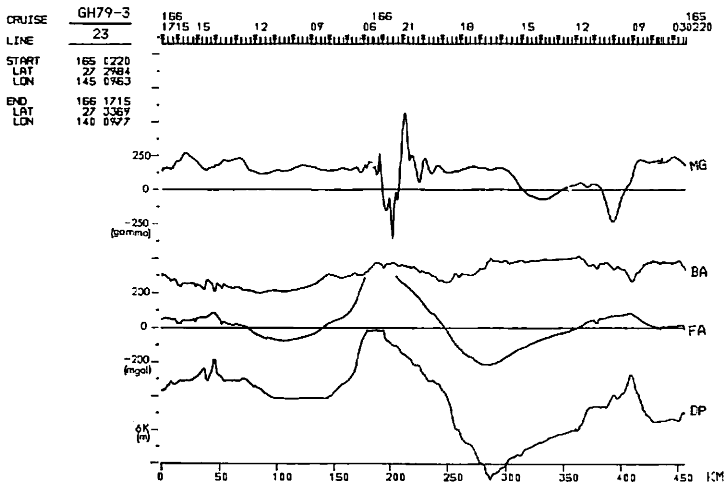
CRUISE GH79-3
LINE 23
START 165 0220
LAT 27 2984
LON 145 0963
END 166 1715
LAT 27 3369
LON 140 0977
166 1715 15 12 09 06 166 21 18 15 12 09 165 030220
250
0
-250
(gamma)
MG
200
0
-200
(mgal)
BA
FA
6K
(m)
DP
0 50 100 150 200 250 300 350 400 450 KM

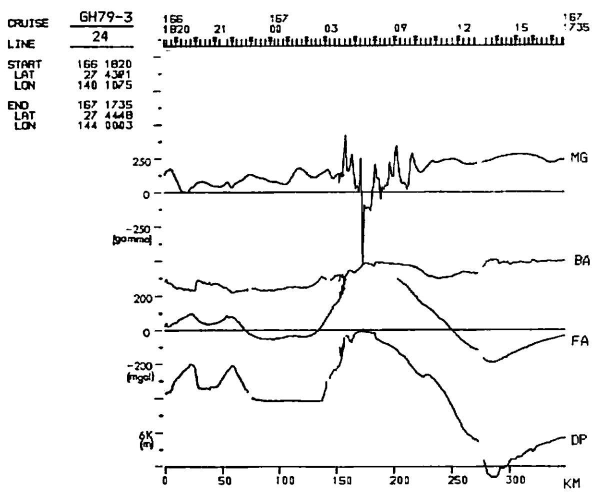
CRUISE GH79-3
LINE 24
START 166 1820
LAT 27 4391
LON 140 1075
END 167 1735
LAT 27 4448
LON 144 0003
166 1820 21 167 00 03 09 12 15 167 1735
250
0
-250
(gamma)
MG
200
0
-200
(mgal)
BA
FA
6K
(m)
DP
0 50 100 150 200 250 300 KM

Fig. IV-4 (M)

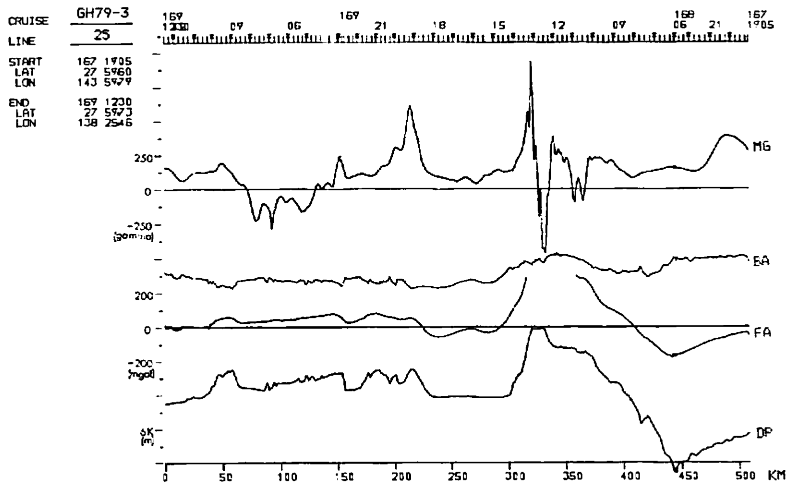
CRUISE GH79-3
LINE 25
START 167 1905
LAT 27 5960
LON 143 5979
END 169 1230
LAT 27 5973
LON 138 2546
MG
BA
FA
DP
KM

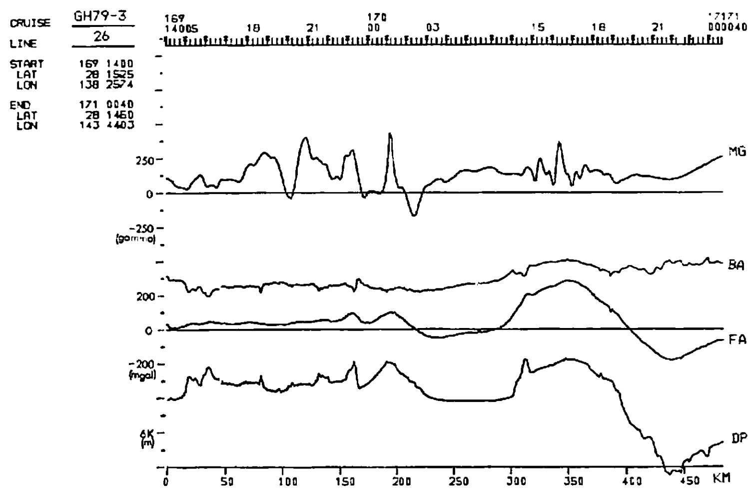
CRUISE GH79-3
LINE 26
START 169 1400
LAT 28 1525
LON 138 2574
END 171 0040
LAT 28 1460
LON 143 4403
MG
BA
FA
DP
KM

Fig. IV-4 (N)

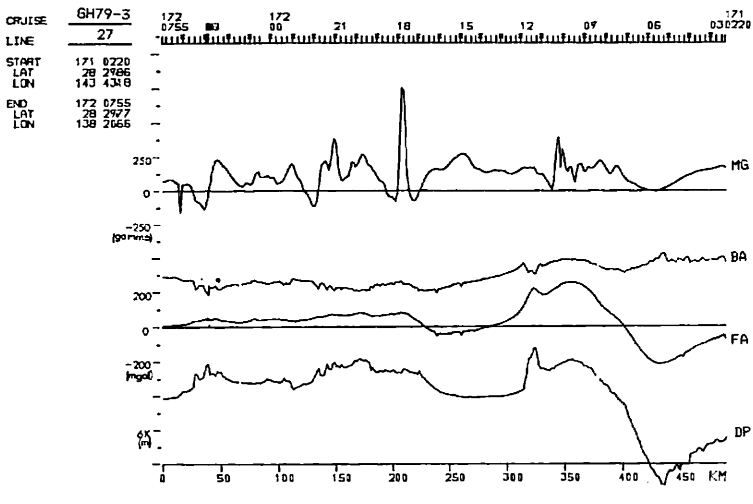

CRUISE GH79-3
LINE 27
START 171 0220
LAT 28 2986
LON 143 4318
END 172 0755
LAT 28 2977
LON 138 2066
MG
BA
FA
DP
KM

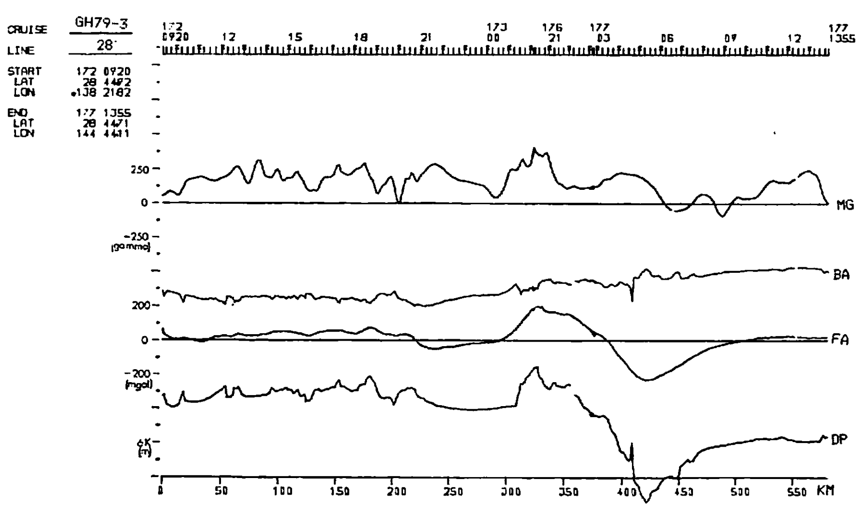

CRUISE GH79-3
LINE 28
START 172 0920
LAT 28 4472
LON 138 2182
END 177 1355
LAT 28 4471
LON 144 4411
MG
BA
FA
DP
KM

Fig. IV-4 (O)

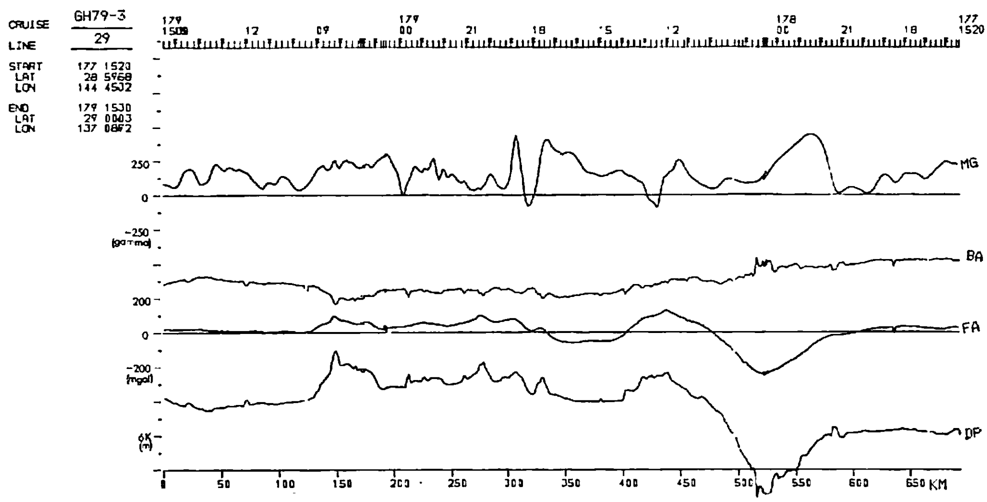
CRUISE
GH79-3
LINE
29
START
LAT
LON
177 1520
28 5968
144 4502
END
LAT
LON
179 1530
29 0003
137 0872
MG
BA
FA
DP
250
0
-250
(gamma)
200
0
-200
(mgal)
KM

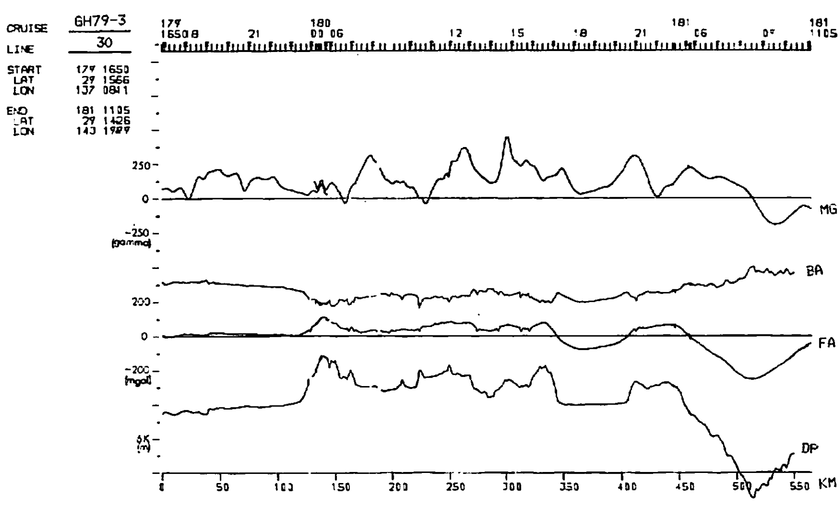
CRUISE
GH79-3
LINE
30
START
LAT
LON
179 1650
29 1566
137 0841
END
LAT
LON
181 1105
29 1426
143 1979
MG
BA
FA
DP
250
0
-250
(gamma)
200
0
-200
(mgal)
KM

Fig. IV-4 (P)

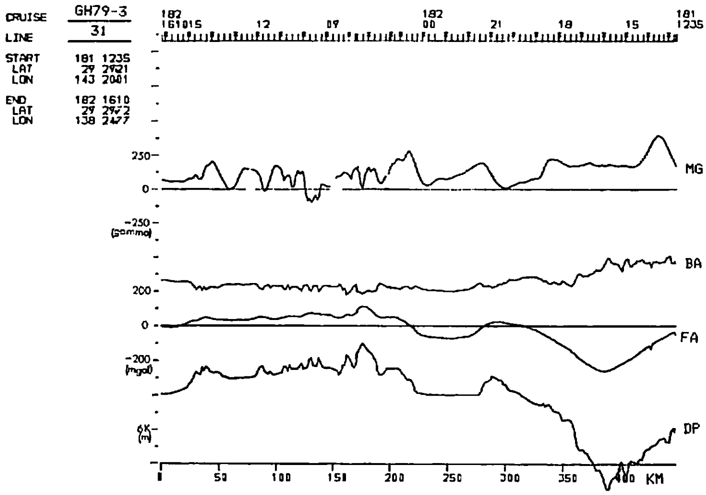
CRUISE GH79-3
LINE 31
START 181 1235
END 182 1610
MG
BA
FA
DP
KM

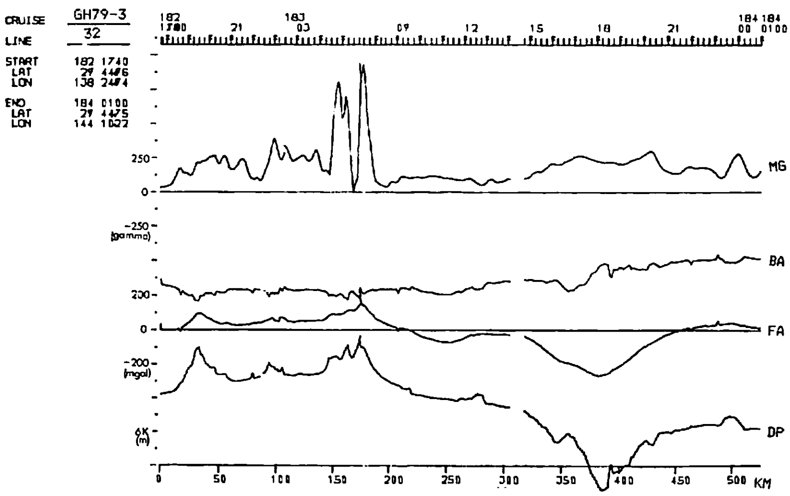
CRUISE GH79-3
LINE 32
START 182 1740
END 184 0100
MG
BA
FA
DP
KM

Fig. IV-4 (Q)

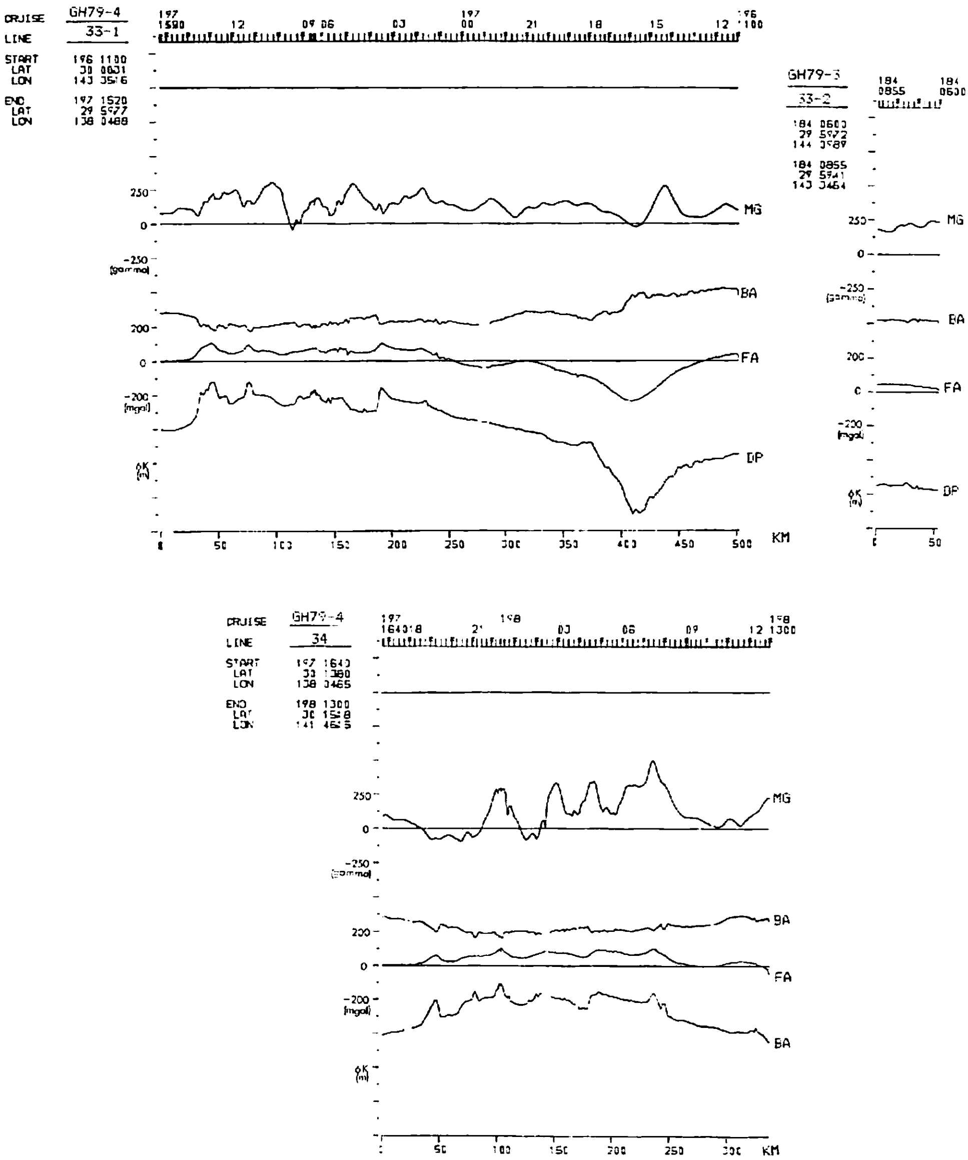
CRUISE GH79-4
LINE 33-1
START 196 1100
END 197 1520
MG
BA
FA
DP
KM
GH79-3
33-2
CRUISE GH79-4
LINE 34
START 197 1640
END 198 1300
MG
BA
FA
BA
KM

Fig. IV-4 (R)

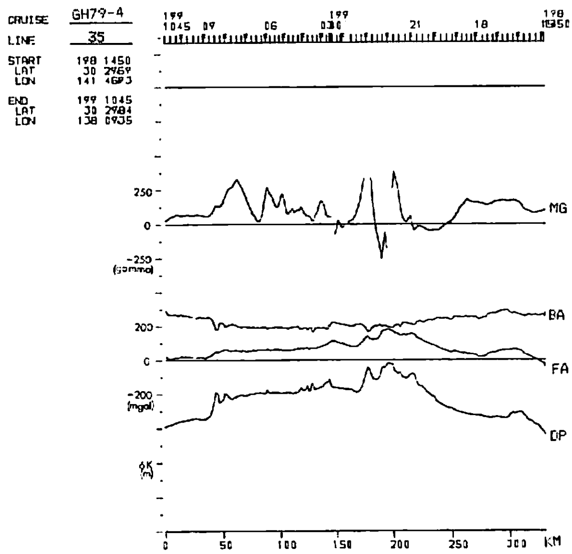
CRUISE GH79-4
LINE 35
START 198 1450
LAT 30 2969
LON 141
END 199 1045
LAT 30
LON 138
250
0
-250
(gamma)
MG
200
0
-200
(mgal)
BA
FA
DP
0 50 100 150 200 250 300 KM

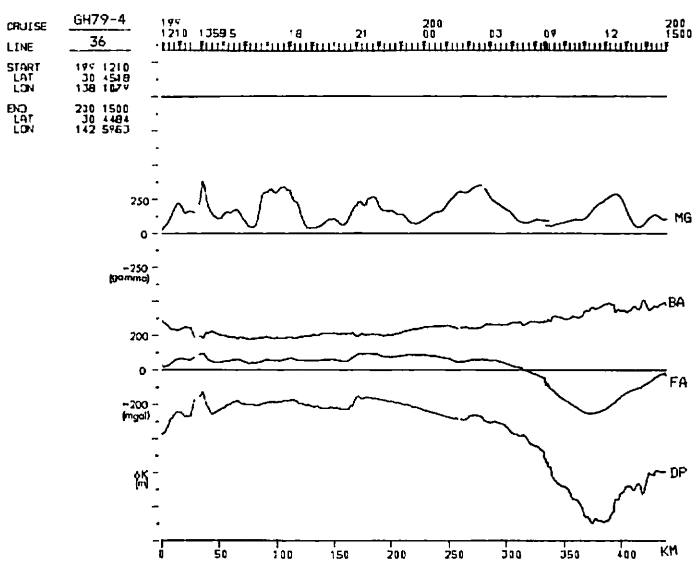
CRUISE GH79-4
LINE 36
START 1210
LAT 30
LON 138
END 1500
LAT 30 4484
LON 142
250
0
-250
(gamma)
MG
200
0
-200
(mgal)
BA
FA
DP
0 50 100 150 200 250 300 350 400 KM

Fig. IV-4 (S)

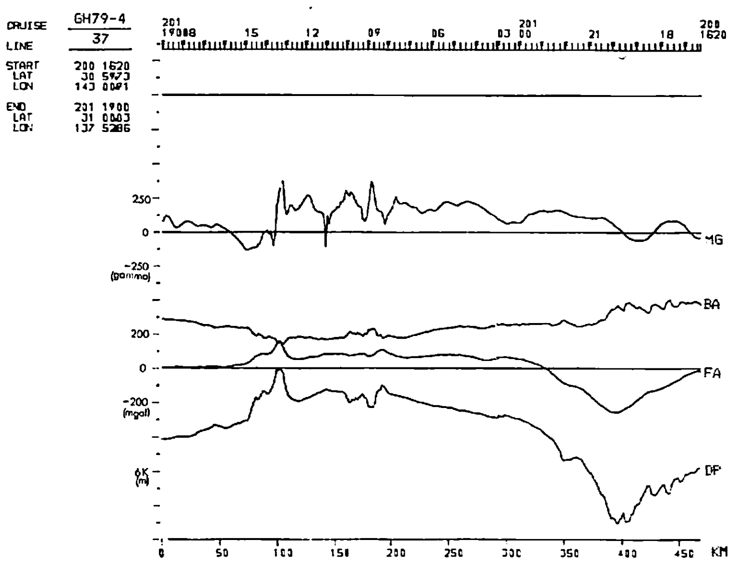
CRUISE
GH79-4
LINE
37
START
LAT
LON
END
LAT
LON
250
0
-250
(gamma)
MG
BA
200
0
-200
(mgal)
FA
DP
KM

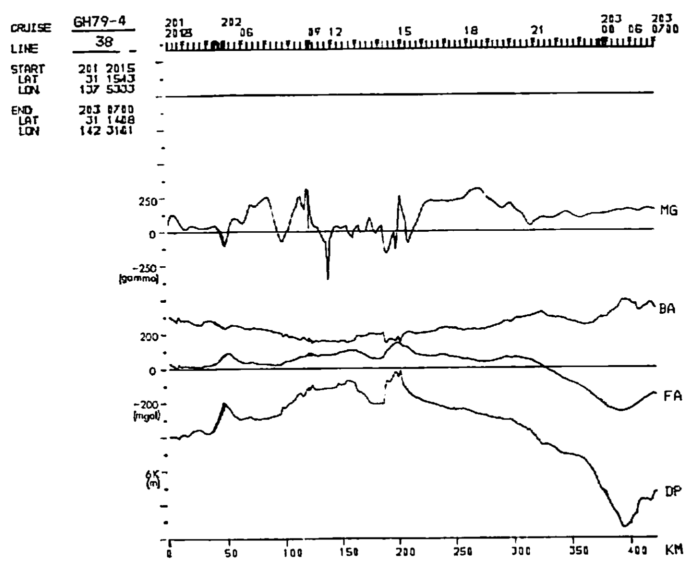
CRUISE
GH79-4
LINE
38
START
LAT
LON
END
LAT
LON
250
0
-250
(gamma)
MG
BA
200
0
-200
(mgal)
FA
DP
KM

Fig. IV-4 (T)

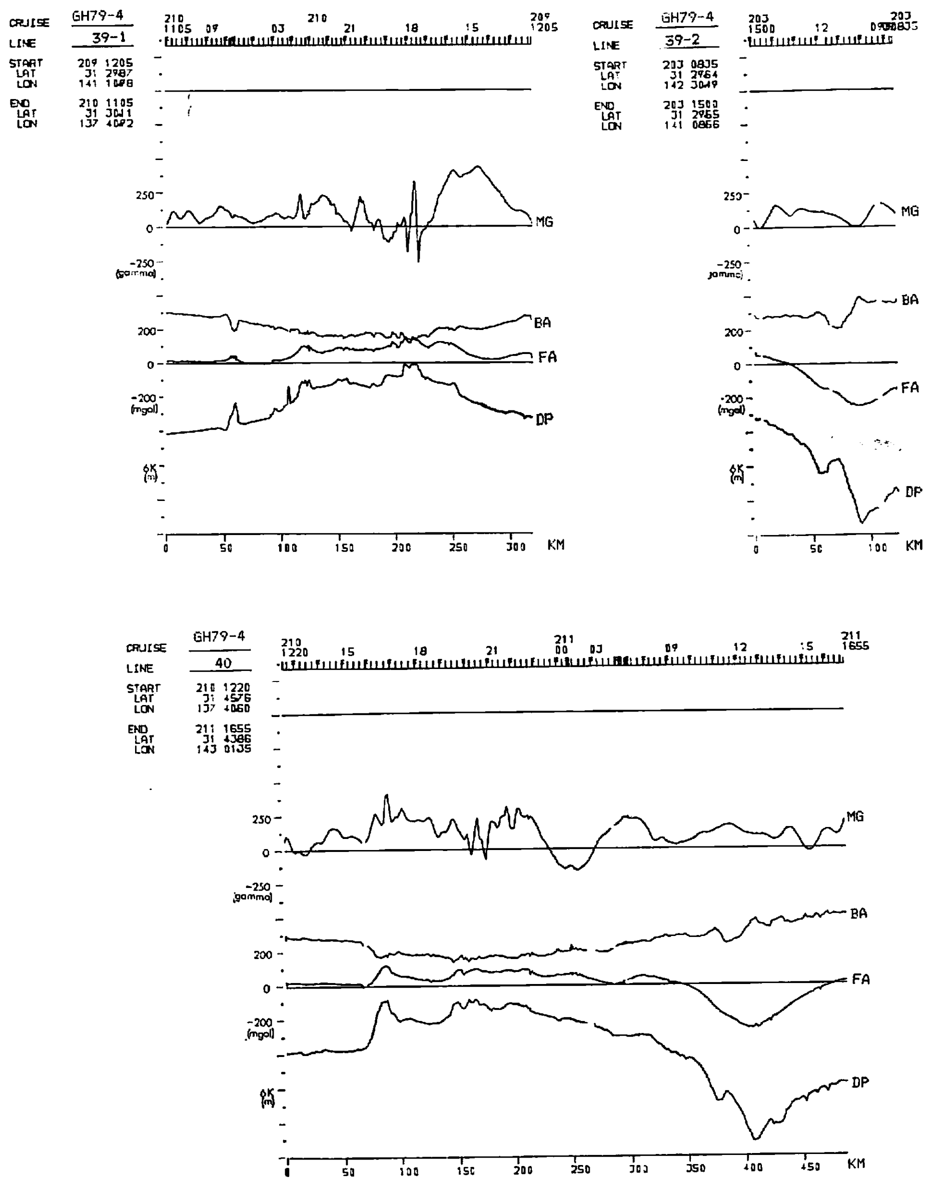
CRUISE GH79-4
LINE 39-1
START
LAT
LON
END
LAT
LON
MG
BA
FA
DP
(gamma)
(mgal)
KM
CRUISE GH79-4
LINE 39-2
START
LAT
LON
END
LAT
LON
MG
BA
FA
DP
KM
CRUISE GH79-4
LINE 40
START 210 1220
LAT 31 4576
LON 137 4060
END 211 1655
LAT 31 4386
LON 143 0135
MG
BA
FA
DP
(gamma)
(mgal)
KM

Fig. IV-4 (U)

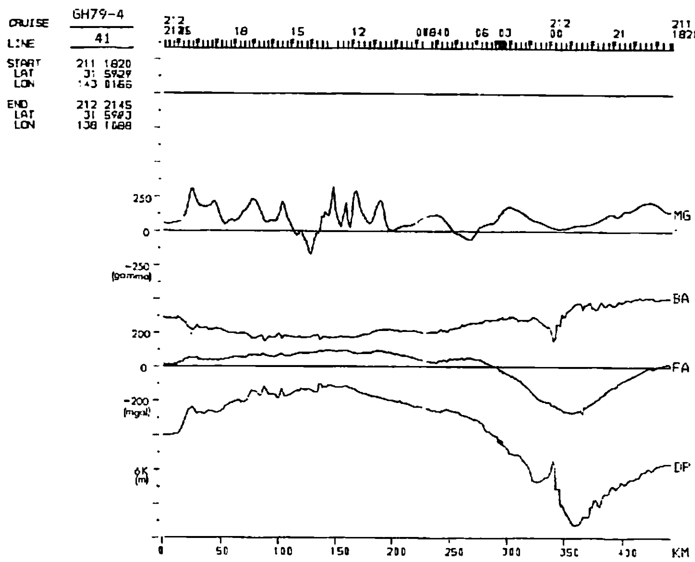
CRUISE
GH79-4
LINE
41
START
LAT
LON
211 1820
END
LAT
LON
212 2145
MG
BA
FA
DP
250
0
-250
(gamma)
200
0
-200
(mgal)
KM

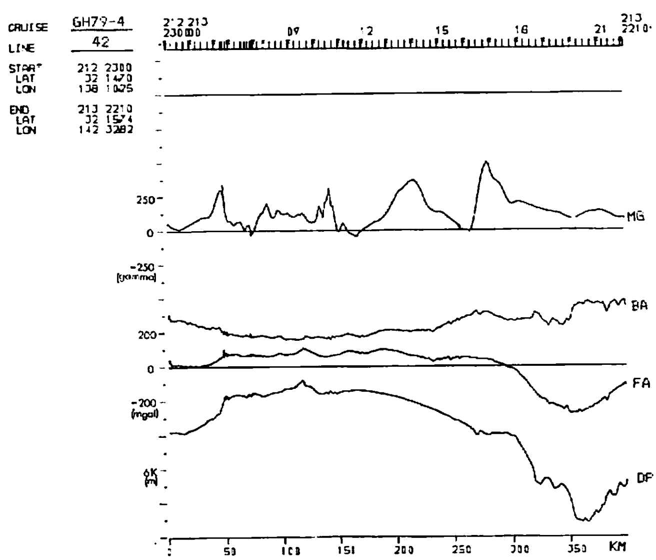
CRUISE
GH79-4
LINE
42
START
LAT
LON
212 2300
END
LAT
LON
213 2210
MG
BA
FA
DP
250
0
-250
(gamma)
200
0
-200
(mgal)
KM

Fig. IV-4 (V)

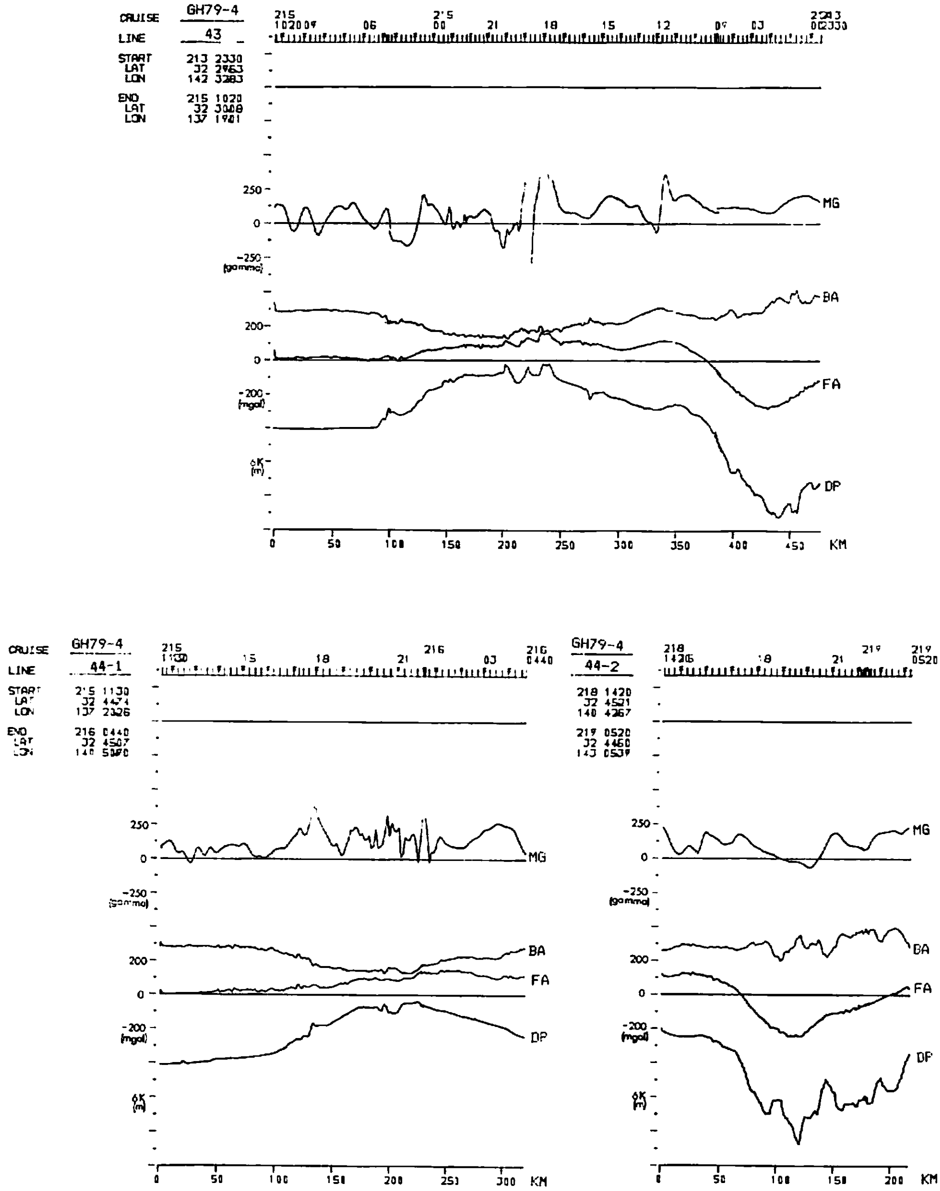
CRUISE
GH79-4
LINE
43
START
LAT
LON
END
LAT
LON
MG
BA
FA
DP
(gamma)
(mgal)
KM
CRUISE
GH79-4
LINE
44-1
START
LAT
LON
END
LAT
LON
MG
BA
FA
DP
KM
GH79-4
44-2
MG
BA
FA
DP
KM

Fig. IV-4 (W)

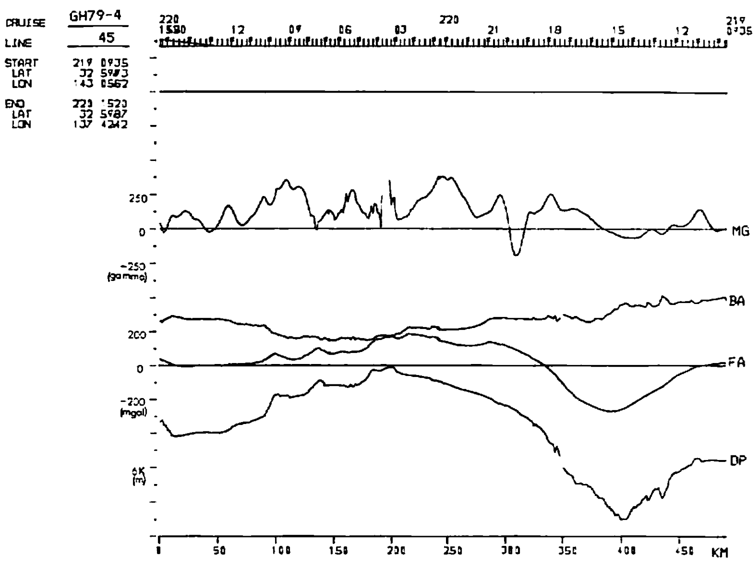
CRUISE GH79-4
LINE 45
START 219 0935
END
MG
BA
FA
DP
(gamma)
(mgal)
0 50 100 150 200 250 300 350 400 450 KM

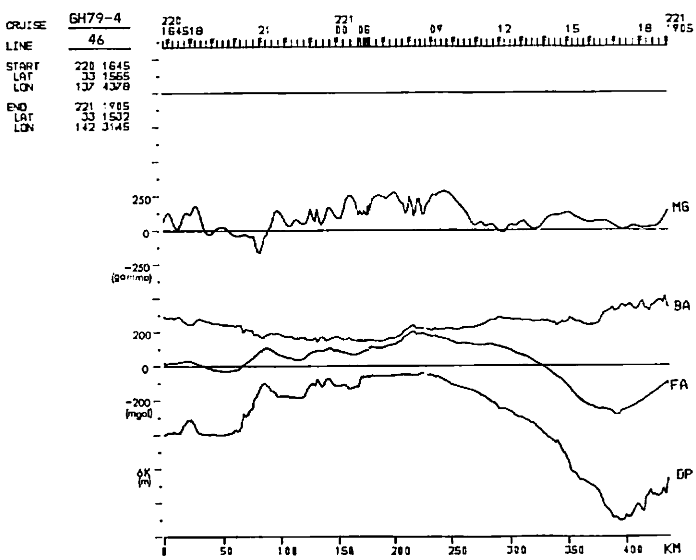
CRUISE GH79-4
LINE 46
START 220 1645
END 221 1905
MG
BA
FA
DP
(gamma)
(mgal)
0 50 100 150 200 250 300 350 400 KM

Fig. IV-4 (X)

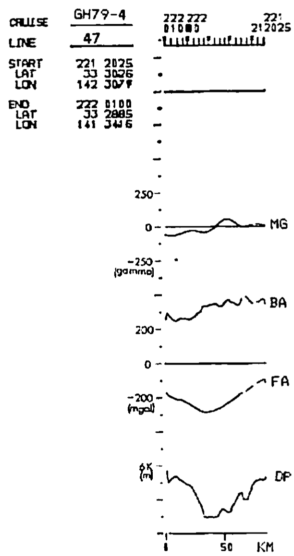
CRUISE GH79-4
LINE 47
START 221 2025
LAT 33 3026
LON 142 3079
END 222 0100
LAT 33 2885
LON 141 3446
MG
BA
FA
DP
50 KM

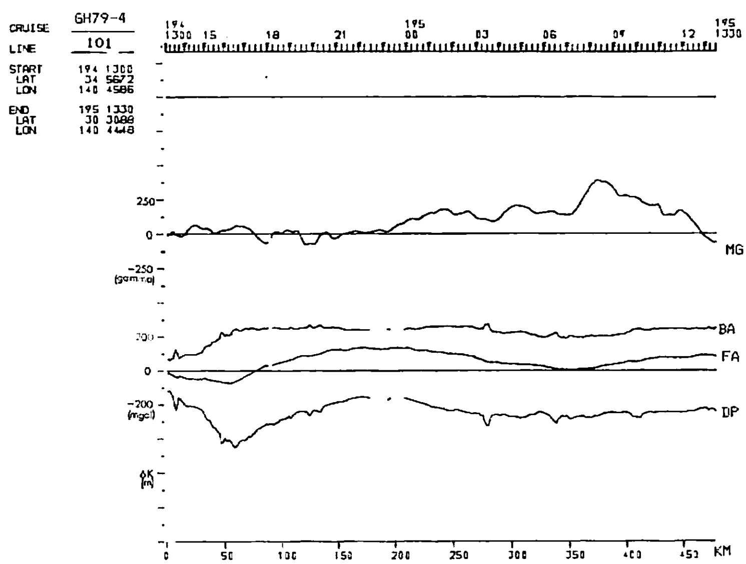
CRUISE GH79-4
LINE 101
START 194 1300
LAT 34 5672
LON 140 4586
END 195 1330
LAT 30 3088
LON 140 4448
MG
BA
FA
DP
KM

Fig. IV-4 (Y)

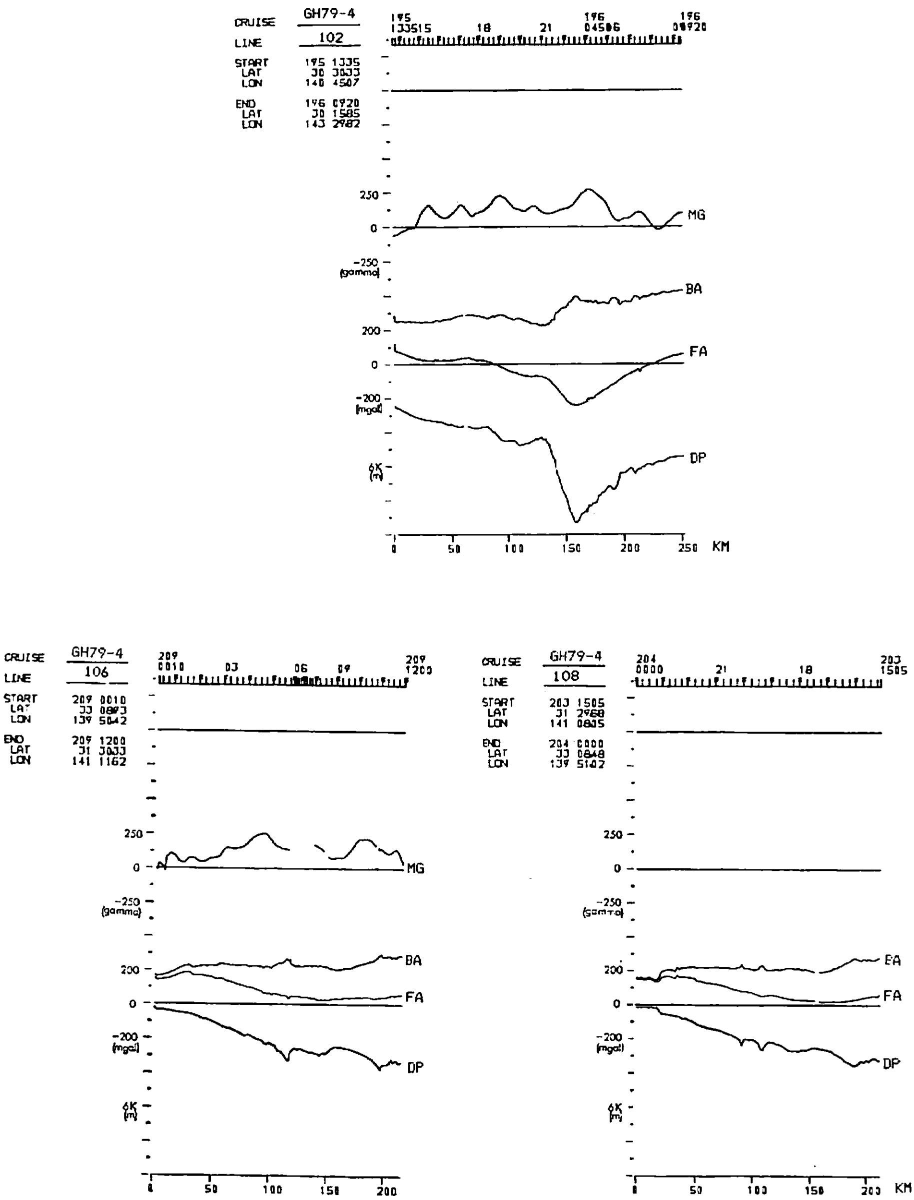
CRUISE GH79-4
LINE 102
START 195 1335
LAT 30 3033
LON 140 4507
END 196 0920
LAT 30 1585
LON 143 2982
MG
BA
FA
DP
(gamma)
(mgal)
6K (m)
0 50 100 150 200 250 KM
CRUISE GH79-4
LINE 106
START 209 0010
END 209 1200
LAT 31 3033
LON 141 1162
CRUISE GH79-4
LINE 108
START 203 1505
LAT 31 2968
LON 141 0805
END 204 0000
LAT 33 0848
LON 139 5102
KM

Fig. IV-4 (Z)

The Ogasawara Trough east of the Shichito Ridge is associated with a negative anomaly belt which extends between the Ogasawara and the Shichito Ridges and parallel to them from about 30°N to 25°N. Though the sea water is deepest in the northern part of the trough, the minimum values of free air anomalies occur southwest of Hahajima Island. This suggests that low density sediments thicken southward along the trough.

The Ogasawara Ridge is characterized by a large-amplitude belt of positive anomalies. The maximum values of free air anomalies (up to +380 mgal) occur in the northern part of the Ogasawara Islands. This positive belt seems to extend southward into the trench slope break area west of the Mariana Trench down to 24°N, although anomaly values over the trench slope break area are of much lower amplitude (in the range of +80 to +100 mgal).

The amplitude of negative anomalies associated with the Mariana Trench decreases northward, and free air anomaly values of about −50 mgal occur at the junction of the Mariana and the Ogasawara Trenches. Two minima occur in the Ogasawara Trench: a minimum of −225 mgal east of Chichijima Island, and another of −270 mgal at about 30°N.

A few small scale gravity lows with minima of +30 mgal occur just west of the Shichito Ridge. Further to the west there is a basin associated with flat anomalies in the range of +30 to +60 mgal. At around 27°N, the Bouguer anomalies in this basin are approximately 100 mgal higher than those in the Ogasawara Trough (e.g. L22, Fig. IV-4), which suggests that the deep structures in these two areas are quite different. At the border between this basin and the Shikoku Basin, there are no prominent high anomalies which may be associated with the Izu Ridge. Free air anomalies along this border reach +60 mgal in places.

The Torishima-Smithjima Region [lat 30°N to lat 32°N, L33 to L41, Fig. IV-4]

This region is a broad area with water depths less than 2000 m. Because of its relatively high elevation, the average free air anomaly value in this region is higher than in the Ogasawara-Iwojima region, although there are no prominent positive anomalies as there are over the Ogasawara Ridge.

Torishima and Smithjima Islands have associated anomaly maxima of up to +200 and +150 mgal, respectively. Another anomaly maximum of +70 mgal occurs over the trench slope break east of the Shichito Ridge. There is a low anomaly belt having a minimum value of +10 mgal between the ridge and the trench slope break area, which suggests the presence of thick sediment layers in this area.

The gravity anomalies west of the Shichito Ridge are complicated. The Izu Ridge, which extends *en échelon* north-south, is associated with anomaly highs, and free air anomaly values exceed +100 mgal at places along the ridge, while areas between the topographic highs are associated with anomalies as low as +40 mgal.

The Ogasawara Trench is associated with a negative anomaly belt, the amplitude of which increases northward, reaching a maximum of −270 mgal at about 32°N.

The Hachijojima Region [down to lat 32°N, L42 to L47, Fig. IV-4]

The water becomes shallower in this region. An area with free air anomalies higher than +100 mgal extends from Hachijojima Island to the trench slope break area east of it, with maxima greater than +200 mgal occurring northeast of Hachijojima Island. There are no notable anomaly lows between this area of anomaly maxima and the trench slope break area, which suggests either that there are no thick sediments in the area or that the density of the sedimentary rocks is not significantly less than that of the trench slope break area.

The Izu Ridge west of Hachijojima Island is associated with positive anomalies with maxima of +90 mgal.

The Ogasawara Trench is associated with a high-amplitude belt of negative anomalies, with minimum free air anomaly values occurring at the junction of the Ogasawara and Japan Trenches.

Discussion

Free air anomaly values of nearly +400 mgal, which occur over the northern part of the Ogasawara Ridge, are amongst the largest anomalies in the world (WATTS *et al.*, 1976). In order to clarify the source of these anomalies they were compared with the anomalies over the trench slope break north of the ridge. Although the gravity effect of upper mantle heterogeneity, especially that of the descending lithosphere, might be remarkable in an island arc region, this effect is probably not significant between the Ogasawara Ridge and the trench slope break north of it. We neglect this effect in the following discussion.

The gravity effect of each area is approximated by the simple and well-known infinite horizontal slab model:

$$g = 2\pi G\rho h, \qquad (1)$$

where g is the gravity effect due to a source layer with a thickness h and a density ρ, and $G (= 6.672 \times 10^{-8}\ \mathrm{cm^3\ gr^{-1}\ sec^{-2}})$ is the gravitational constant. If we only consider the difference in water depth, the difference of free air anomaly values of both areas can be derived from equation (1):

$$\delta g = 2\pi G(\rho_1 - \rho_2)h, \qquad (2)$$

where $\rho_2 (= 1.03\ \mathrm{gr/cm^3})$ is the sea water density and ρ_1 is the density of the replaced material. Free air anomalies over the northern part of the Ogasawara Ridge are approximately 350 mgal greater than those over the trench slope break at 32°N, while the water depth in the former region is about 2.5 km less than in the latter. By substituting h = 2.5 km and $\delta g = 350$ mgal, we obtain the density of the replaced material $\rho_1 = 4.4\ \mathrm{gr/cm^3}$, which is an unusually high density for material in the crust or the upper mantle. If we substitute $\rho_1 = 3.3\ \mathrm{gr/cm^3}$ instead of 4.4 gr/cm³ equation (2) gives $\delta g = 240$ mgal, which is the gravity difference due to the difference in water depth between both regions assuming the same crustal thickness and the same crustal mean density for each.

The observed gravity difference is, however, 110 mgal greater than the above value. Two simple crustal models for the Ogasawara Ridge in comparison with a crustal model for the trench slope break north of it (column A) are shown in Fig. IV-5. The column B shows a crustal thinning model. If we suppose the upper

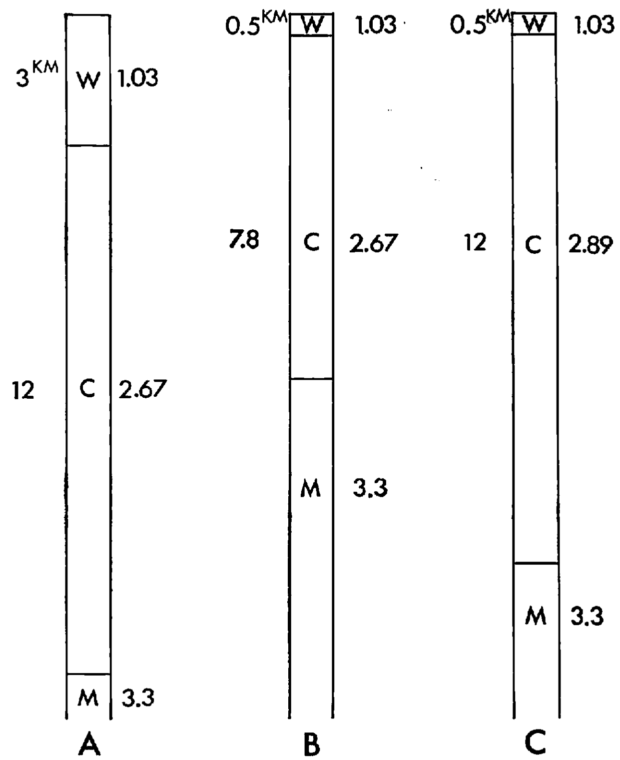

Fig. IV-5 Simple crustal models for trench slope break at 32°N (A) and for the Ogasawara Ridge (B, C). Figures on the left and right side of each column indicate thicknesses and densities respectively. W, sea water; C, crust; M, upper mantle.

mantle density ρ_1 and the mean crustal density ρ_2 to be 3.3 and 2.67 gr/cm^3 respectively, the difference in crustal thickness between the areas is obtained by equation (2) with $\delta g = 110$ mgal: $h = 4.2$ km. The result indicates that the Mohorovicic Discontinuity under the Ogasawara Ridge exists about 8 km below sea level, or is 6.7 km shallower than at 32°N, where a seismic refraction experiment indicated that the Moho there is located about 15 km below sea level (HOTTA, 1972).

An alternative interpretation for the anomalous high gravity anomalies over the Ogasawara Ridge is a high-density crust model (column C in Fig. IV-5). If the crustal thickness is 12 km, the difference in mean crustal density between the two areas can be obtained from equation (2): $\rho_1 - \rho_2 = 0.22$ gr/cm^3. If the crustal density is assumed to be 2.67 gr/cm^3 under the trench slope break at 32°N, this result implies that it is 2.89 gr/cm^3 under the Ogasawara Ridge, which is a little high as a mean crustal density, but would be possible if the crust were mainly composed of, for example, gabbro. In favour of these models is the presence of boninite on the Ogasawara Ridge. It seems to be likely that the same mechanism that resulted in the formation of boninite also led to a high density and/or thin crust here.

References Cited

FUJII, Y., KOGURE, S. and KITADA, K. (1964) Gravity survey in Hachijō and Torishima Islands. *J. Geodetic Soc. of Japan*, vol. 10, p. 24–35.

Geographical Survey Institute (1976) Establishment of the Japan Gravity Standardization Net 1975. *J. Geodetic Soc. of Japan*, vol. 22, p. 65–76.

HOTTA, H. (1970) A crustal section across the Izu-Ogasawara Arc and Trench. *J. Phys. Earth*, vol. 18, p. 125–141.

ISHIHARA, T. (1976) Gravity measurement on traverse line across Izu-Ogasawara Arc and Trench. *Izu-Ogasawara (Bonin) Arc and Trench Investigations. Geol. Surv. Japan Cruise Rept., no. 5*, p. 24.

MIYAZAKA, T. (1979) Gravity Survey. *Geological Investigation of the Japan Sea. Geol. Surv. Japan Cruise Rept.*, no. 13, p. 27–45.

NETTLETON, L. L. (1976) *Gravity and Magnetics in Oil Prospecting*, McGraw-Hill Book Company, New York.

OHKAWA S. and YOKOYAMA I. (1977) Gravity anomalies on Nishinoshima Volcano. *Geophys. Bull. of Hokkaido Univ.*, vol. 36, p. 83–95.

SEGAWA, J. and BOWIN, C. (1976) Gravity in the Junction between the Japanese and the Izu-Bonin Islands. *J. Phys. Earth*, vol. 24, p. 275–311.

SEGAWA, J. and TOMODA, Y. (1976) Gravity measurements near Japan and study of the upper mantle beneath the oceanic trench-marginal sea transition zones. in *The Geophysics of the Pacific Ocean Basin and Its Margin, Geophys. Monogr. Ser.*, vol. 19, p. 35–52, American Geophys. Union, Washington, D.C.

TANAKA, M., HOSONO, T., KUBOKI, T., OWADA, S. and TACHIKAWA, T. (1974) Geomagnetic and gravity surveys in the Bonin Island (Chichijima), the Ogasawara Archipelago. *J. Geodetic Soc. of Japan*, vol. 20, p. 193–208.

TOMODA, Y. (1973) *Maps of Free Air and Bouguer Gravity Anomalies in and around Japan*. Univ. Tokyo Press.

WATTS, A. B. (1976) *Gravity Field of the Northwest Pacific Ocean Basin and Its Margin: Philippine Sea*, Geol. Soc. America Map and Chart Ser. MC-12.

WATTS, A. B., TALWANI, M. and COCHRAN, J. R. (1976) Gravity field of the northwest Pacific ocean basin and its margin. in *The Geophysics of the Pacific Ocean Basin and Its Margin, Geophys. Monogr. Ser.*, vol. 19, p. 17–34, American Geophys. Union, Washington, D.C.